On the Use of Frequency-diversity for Efficient Wireless Power Transmission

D. Masotti * (1), E. Fazzini (1), and A. Costanzo(2)
(1) DEI-University of Bologna, Bologna Campus, Italy
(2) DEI-University of Bologna, Cesena Campus, Italy

Abstract

In this paper a wide and deep analysis of the complex radiating mechanism of frequency diverse arrays (FDAs) is provided, by highlighting the strict relationship between the angle, range and time dependency of the corresponding radiation performance. The capability to focus the signal/power in a prescribed region of the space is obtained at the expense of a tough architectural complexity which makes FDAs a pure theoretical topic, up to now. A solution for the practical exploitation of FDAs for wireless power transfer application is the main goal of this paper.

1 Introduction

The far-field wireless transfer of power (WPT) is a challenging research topic whose main obstacle, from the practical realization point of view, is the low efficiency of the entire link, from the dc power used to bias and energize the transmitting side, up to the dc power actually delivered to the receiver load. The least efficient block of this chain is the radio-frequency transmitting source: this poor behavior is not a matter of the components of the transmitter itself (i.e., oscillator, amplifier, and antenna), but of the philosophy which the transmission is based on. Standard transmitting phased-arrays are highly efficient radiating architectures able to selectively send the power only in a prescribed angle direction; similarly, Bessel and/or Gaussian beam-launcher are structures able to convey the signal/power in a transversally-controlled region, but limited to the near-field region [1-2].
The capability to select also the far-field distance where the energy has to be concentrated is peculiar to frequency-diverse arrays (FDAs), where the different frequencies radiated by the array elements make this possible [3].
Aim of this contribution is to deeply investigate the complex behavior of these radiating systems, and to pave the way to their practical exploitation for WPT purposes. In order to reach this goal, a bi-dimensional array operating at millimeter (mm)-wave is considered as a future smart power transmitter for Internet-of-Things (IoT) applications.

2 Effect of the frequency diversity

In order to quantify the impact of the frequency diversity on the radiation performance of an array, let us consider a mm-wave array of 16 x 16 patch antennas. All the antennas are square patch resonating at 24 GHz, realized on a Rogers RO3003 substrate (ε_r=3.02, tanδ=0.0016, thickness=0.254 mm), with an edge length of 3.56 mm (see Fig. 1). As previously explained, the choice of the mm-wave range is made because energy focusing for future battery-less IoT devices is a mandatory requirement. However, all the considerations made in the following apply for microwave applications, too.

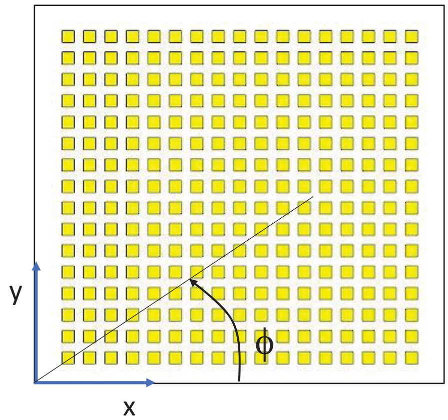

Figure 1. Layout of a planar 16 x 16 patch array, on a Rogers RO3003 substrate, for WPT at 24 GHz.

The aim of this Section is to verify the effect of the radiation of different frequencies by the array elements. The most general situation is that each patch antenna has its own frequency, hence the signal in a specific far-field point (r, θ, ϕ) (with respect to the phase center of the element in position (0,0) of the array) can be cast in the following way:

$$s(t) = \sum_{n=0}^{15}\sum_{m=0}^{15} b_{m,n} exp\left(j2\pi f_{m,n}\left(t-\frac{R_{m,n}}{c}\right)\right) \quad (1)$$

where $b_{m,n}$ is the complex excitation coefficient of the generic (m, n) patch of the array (in the following considered all equal to unity, for simplicity), c is the speed of light, $f_{m,n}$ and $R_{m,n}$ are the corresponding radiated frequency and far-field range, respectively. The last one can be easily evaluated after some algebraic calculations. As per $f_{m,n}$, the following simple expression holds:

$$f_{m,n} = f_{0,0} + (m-1)\Delta f + (n-1)\Delta f \qquad (1)$$

where $f_{0,0}$ =24 GHz, Δf is the (constant, in this case) frequency shift, equal to 5 MHz in the following examples.
The array factor can be obtained from (1) by dividing it by the basis (position (0,0)) element contribution: one can note that the corresponding expression becomes dependent not only on the angular position (inside $R_{m,n}$ expression) as in standard phased-array, but also on the range r (again inside $R_{m,n}$), and finally on time (t).
Let us start from the simpler case where each column of the array has the same frequency: this means that in (1) $f_{m,n}$ is replaced by $f_m = 24GHz + (m-1)5MHz$. This solution is significantly simpler form the excitation point of view, because the envisaged Software Defined Radio (SDR) responsible for driving the FDA has to have just 16 output channels. In this case the beam-pattern (i.e., the squared magnitude of the array factor) plot assumes the shapes given in Fig. 2, where the pattern in the planes ϕ=90°, ϕ=45°, and ϕ=0° are reported. Note that those plots include the full-wave contribution of the array of Fig. 1.
From figures inspection, one can note that the focusing (in the θ=0° direction and at the distance r=30 m, in this case) is excellent in the first two planes, but it assumes the typical (for FDAs) “S” shape [4] in the ϕ=0°, hence in the plane where frequency-diversity is applied. The S-shape means that, in the plane where it occurs, the focusing capability is not completely controlled, because the maximum is “moving” in the (r, θ) plane, hence the target point (r, θ)=(30m, 0°) is not the sole achieved point. But this happens in that plane, only.

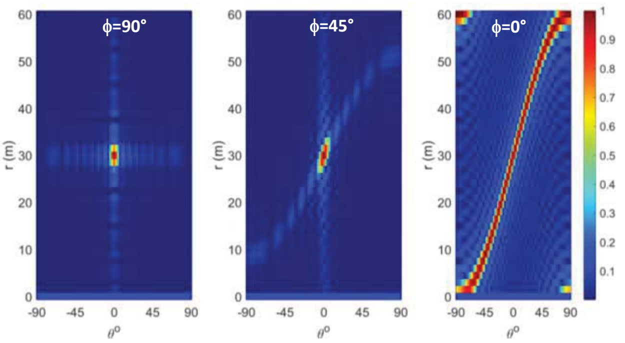

Figure 2. Beam-pattern of the patch array of Fig. 1 in the ϕ=90°, 45°, 0° planes, when $f_{0,0}$=24 GHz, Δf=5 MHz, and each element of a column of the array shares the same frequency (frequency-diversity is applied to array rows, only) .

If the complexity of the array is significantly increased by considering the frequency diversity in both rows and columns of the array (hence, 256 independent channels to be controlled), the corresponding plots of the beam pattern are shown in Fig. 3. It is worth noticing that, despite the increase of the system complexity, the S-shape is still present, this time in the ϕ=45° plane.

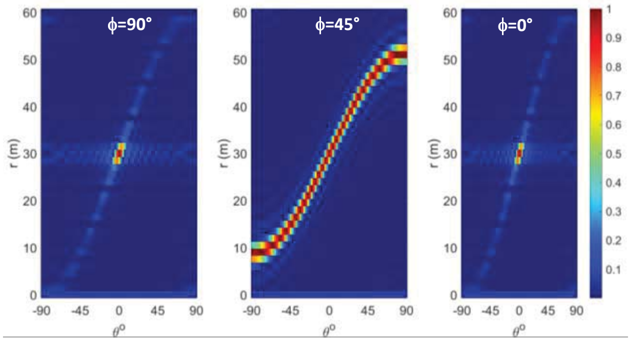

Figure 3. Beam-pattern of the patch array of Fig. 1 in the ϕ=90°, 45°, 0° planes, when $f_{0,0}$=24 GHz, Δf=5 MHz, and each element of the array has its own frequency (frequency-diversity is applied to both columns and rows of the array).

This represents an interesting and novel outcome of this investigation: according to these results, it is not necessary to invest on an excessive complexity of the array in terms of frequency diversity. The problem can be partially improved by resorting to a logarithmic distribution of the element spacings in the array [5], because the S-shape is smoothed. As an alternative, the spot of the beam-pattern is guaranteed in all the planes if a complex optimization algorithm is run by playing with the complex excitation coefficients $b_{m,n}$ [6].
Therefore, FDAs can be effective for power focusing, even with driving architecture not extremely complex.

3 Control of the time-dependency

The complexity of the radiative behaviour of FDA is further emphasized by another problem which is often neglected in the literature, related to the time-dependency of the beam-pattern. This means that, even in the right plane (e.g., the ϕ=90° one in the previous examples) the maximum of radiation is linearly moving with time, as (1) also suggests. This issue can be practically solved by following the indication preliminary given in [7] and widely explained in this paper. As can be seen in Fig. 4(a), showing the beam-pattern of the case of Fig. 2 (but identical behaviour is obtained when the frequency diversity is applied at all the array elements) vs. time, the maximum at 30 m of the previous examples is obtained when the time is exactly 100 ns within the FDA time-period $T = 1/\Delta f$ = 200 ns. In fact, the plots of Figs. 2, 3 have been obtained by placing t=100 ns in (1).
This means that the only way one has for the practical use of FDAs for beam focusing is to resort to the previously mentioned strategies (i.e., the logarithmic inter-element space distribution and/or the complex coefficients $b_{m,n}$ optimization) together with the novelty of this paper, consisting in time controlling the excitations through

delayed rectangular pulses $u(t-\tau)$. These pulses must be kept always zero except for a narrow time window centred around the desired time instant: if the maximum at 30 m is needed, a pulse with a time window around τ=100 ns must periodically (with period $T=1/\Delta f$=200 ns, in this case) drive all the elements of the FDA. Fig. 4(a) superimposes the normalized rectangular pulse (referred to the right y-axis) to the beam-pattern. Of course, a high power peak will be sent in the short time window in such a way to have the required mean power level in the period. From Fig. 4 it is easy to find the rule that maps the time window onto the desired maximum range: for instance, if τ=50 ns the maximum will be at 15 m. The width $\Delta\tau$ of the time window centered around τ is an additional control parameter that allows to shape the dimension of the spot with respect to time in the tri-dimensional space (r, θ, t): Fig. 4(b) shows the corresponding 3D plot of the beam-pattern when τ=100 ns and $\Delta\tau$=20 ns

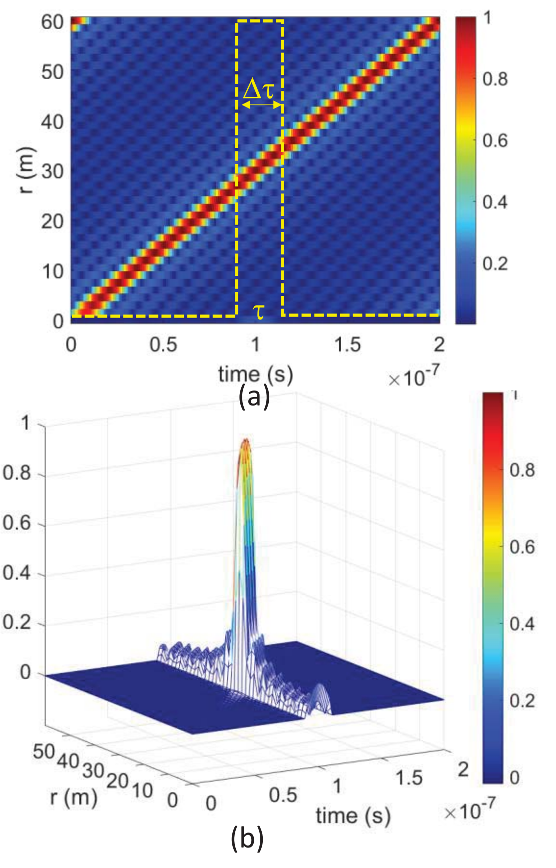

Figure 4. Time-control strategy of the FDA of Fig. 1 with frequency-diversity for rows, only. (a) beam-pattern vs. time of a standard FDA with the superposition of the normalized rectangular pulse; (b) 3D beam-pattern when the time control is applied.

4 Conclusion

The potentialities of FDAs have been highlighted in this paper. The unique capability of simultaneous angle and range selection makes these arrays a promising power source. However, their practical implementation for WPT applications should be limited by the unavoidable change of position of the focusing zone with time. The proposed time-control of the array excitation ports through an SDR represents a viable solution to FDAs exploitation for battery-less devices energization.

5 Acknowledgements

This work was funded by the Italian Ministry of Education, University and Research (MIUR) within the framework of the PRIN 2017-WPT4WID ("Wireless Power Transfer for Wearable and Implantable Devices") ongoing project.

6 References

1. J. D Heebl, M. Ettorre, and A. Grbic, “Wireless Links in the Radiative Near Field via Bessel Beams”, *Phys. Rev. Applied*, **6**, 3, Sept. 2016, pp. 034018, doi: 10.1103/PhysRevApplied.6.034018.

2. W. Fuscaldo, A. Benedetti, D. Comite, P. Baccarelli, Paolo, P. Burghignoli, and A. Galli, “Bessel-Gauss Beams Through Leaky Waves: Focusing and Diffractive Properties”, *Phys. Rev. Applied*, **13**, 6, pp. 064040, June 2020, doi: 10.1103/PhysRevApplied.13.064040.

3. W. Wang, H. C. So, and A. Farina, "An Overview on Time/Frequency Modulated Array Processing," *IEEE Journal of Selected Topics in Signal Processing*, **11**, 2, pp. 228-246, March 2017, doi:10.1109/JSTSP.2016.2627182.

4. D. Masotti, M. Shanawani and A. Costanzo, "Energy Focusing through Layout-based Frequency-Diverse Arrays," *2019 IEEE Wireless Power Transfer Conference (WPTC)*, London, United Kingdom, 2019, pp. 312-315, doi: 10.1109/WPTC45513.2019.9055634.

5. E. Fazzini, M. Shanawani, A. Costanzo and D. Masotti, "Focusing RF-on demand by Logarithmic Frequency-Diverse Arrays," *2020 IEEE Wireless Power Transfer Conference (WPTC)*, Seoul, Korea (South), 2020, pp. 76-79, doi: 10.1109/WPTC48563.2020.9295603.

6. H. Shao, J. Dai, J. Xiong, H. Chen and W. Wang, "Dot-Shaped Range-Angle Beampattern Synthesis for Frequency Diverse Array," *IEEE Antennas and Wireless Propagation Letters*, **15**, pp. 1703-1706, 2016, doi: 10.1109/LAWP.2016.2527818.

7. E. Fazzini, M. Shanawani, A. Costanzo and D. Masotti, "A Logarithmic Frequency-Diverse Array System for Precise Wireless Power Transfer”, presented at *2020 European Microwave Conference (EuMC)*.